

Article

Research on Multi-Objective Optimization Model for Hybrid Energy System Considering Combination of Wind Power and Energy Storage

Jing Wu ¹, Zhongfu Tan ¹, Keke Wang ¹, Yi Liang ^{2,3,*}  and Jinghan Zhou ¹

¹ School of Economics and Management, North China Electric Power University, Changping District, Beijing 102206, China; 1182106009@ncepu.edu.cn (J.W.); tzf@ncepu.edu.cn (Z.T.); 1182106012@ncepu.edu.cn (K.W.); 120192206120@ncepu.edu.cn (J.Z.)

² School of Management, Hebei GEO University, Shijiazhuang 050031, China

³ Strategy and Management Base of Mineral Resources in Hebei Province, Hebei GEO University, Shijiazhuang 050031, China

* Correspondence: louisliang@hgu.edu.cn

Abstract: With the development of renewable energy, the grid connection is faced with great pressure, for its generation uncertainty and fluctuation requires larger reserve capacity, and higher operation costs. Energy storage system, as a flexible unit in the energy system, can effectively share the reserve pressure of the system by charging and discharging behaviors. In order to further improve the renewable energy utilization, the combination of wind power and energy storage for hybrid energy system is proposed. On considering the power generation characteristics, the objective functions are maximizing the system revenue and minimizing the system energy loss. Combined with the robust optimization theory, the model is transformed and solved. The results show that the application of the energy storage will effectively promote the renewable energy consumption, and the combination of the wind power and energy storage will achieve more effective utilization of the night-time wind power and cut down the total system cost.

Keywords: hybrid energy system; combined wind power and energy storage; robust optimization



Citation: Wu, J.; Tan, Z.; Wang, K.; Liang, Y.; Zhou, J. Research on Multi-Objective Optimization Model for Hybrid Energy System Considering Combination of Wind Power and Energy Storage. *Sustainability* **2021**, *13*, 3098. <https://doi.org/10.3390/su13063098>

Academic Editor: Abdollah Shafieezadeh

Received: 30 January 2021

Accepted: 5 March 2021

Published: 11 March 2021

Publisher's Note: MDPI stays neutral with regard to jurisdictional claims in published maps and institutional affiliations.



Copyright: © 2021 by the authors. Licensee MDPI, Basel, Switzerland. This article is an open access article distributed under the terms and conditions of the Creative Commons Attribution (CC BY) license (<https://creativecommons.org/licenses/by/4.0/>).

1. Introduction

With the increasing industrial production and consumption, the coal-oil based traditional energy supply structure now causes serious resource depletion and brings environmental threats [1]. In March 2016, the “13th five-year plan” mentioned that the “Energy Internet” coordinated with source-grid-load-storage would be an important part in the future energy structure [2,3]. The future energy system is supposed to strengthen the coupling and complementation of multiple resources beyond regions and time scales, break the single-layer planning of the original energy system and realize integrated operation [4]. As a flexible element, the energy storage system (ESS) plays a key role in stabilizing the fluctuation of renewable energy getting grid-connection and realizing energy space-time complementarity by power storage and releasing. Considering system scheduling, besides the ESS utilization, the fluctuation of the renewable energy output is also an important issue [5]. In this paper, various loads and the energy conversion are considered, and the combination of wind power and energy storage is proposed to realize the coordinated optimization.

Considering the power output characteristics, scholars have made contributions in solving the uncertainty of renewable energy output. To deal with the generation uncertainty of wind power plant (WPP) and photovoltaic (PV), the Monte Carlo theory was introduced in David. F. et.al (2019) to screen the uncertainty scenarios considering the wind power, electricity price, and load uncertainty, building the simulation under multi-scenario energy system operation [6]. Considering the development uncertainty of the regional multi

energy system, the stochastic programming model was introduced [7]. Dan Z. et.al (2014) and Ke W. et.al (2014) proposed an optimal scheduling model considering uncertainty and demand response through stochastic chance programming and multi-agent method [8,9]. Based on the generation characteristics of renewable energy, Sahand B. et.al (2017) proposed a cross-regional power dispatching optimization model considering generation uncertainty and demand response, which is an important way to balance the power output through the energy consumption habit of the demand side [10].

About the economic dispatching of the multi-energy system (MES), Quan L. et.al (2014) introduced the heat storage device into the energy system and built a comprehensive dispatching model considering the minimum coal consumption of power supply and heating [11]. On considering the transmitting uncertainty of the natural gas, Fei. L. et.al (2019) applied a second-order cone (SOC) relaxation of Weymouth equation to deal with the uncertainty and constructed an economic dispatching optimization model of the MES [12]. Considering the operation constraints and the ESS operation conditions, YX. L. et.al (2018) designed the uncertain regulation parameters and proposed a two-stage robust dispatching optimization model [13].

For MES operation optimization, DiSomma M. et.al (2015) proposed a multi-energy complementary system driven by natural gas, biomass, and PV [14]. Zeng R. et.al (2015) proposed a multi-energy complementary system considering the combined cold and heat power (CCHP) and the ground source heat pump (GSHP) [15]. By introducing a CCHP unit with heat pump, the surplus wind power in the valley period is transformed into heat, and an economic operation model of the microgrid was constructed [16]. Based on the price-based demand response, Ma L et.al (2016) constructed an optimal operation model considering multi-agent joint operation for the microgrid [17]. Taking the annual total cost, annual pollution emission and annual energy consumption as optimization objectives, a multi-objective optimization operation model for a park-level MES was constructed [18]. Combined with the coupling and complementary characteristics of regional cooling, heating and power resources, an optimization model for regional MES was proposed [19].

In addition, the ESS is involved in the smart grid developing. The combination of the WPP and ESS may be a new approach to improve energy utilization and environmental benefits. The joint application of wind power and ESS improves the power characteristic controlling ability when connecting. H.J G et.al (2014) constructed a two-stage model with ESS to obtain more economic benefits by curtailing certain amount of wind power [20]. S.Q Z. et.al (2019) proposed a bi-level programming model of thermal power and energy storage to reduce the fluctuation caused by wind power [21]. ZC. H et.al (2012) proposed an optimization model considering the combination of the pump storage power station [22]. Daneshi H. et.al (2012) presented a model for the hybrid energy system and proposed the detailed unit models and operation constraints [23].

To sum up, research has been made on the complementary operation of the MES, and on the application of ESS in the MES. However, few people analyze the economy of the combined wind power and energy storage. Therefore, considering the economic benefits and energy curtailment, an optimization operation model of the hybrid energy system (HES) considering the combination of WPP and energy storage is proposed. The main contributions of this study are as follows.

- (1) The combined wind power and energy storage is applied as a flexible generator of the HES, which ensures more stable generation of the wind power based on the combined ESS.
- (2) Both system benefits and renewable energy waste are considered in the combined WPP-ESS based hybrid energy system (WEHES). Based on the cost calculation of CHP, wind power plant (WPP), PV, and ESS, a multi-objective hybrid energy system with the maximum benefits and minimum energy waste as the objectives is constructed. Further, the robust optimization and PSO algorithm are used to solve the proposed model.

- (3) In this paper, different scenarios are set up to analyze the economy of combined operation of the HES. By introducing demand response (DR) management to reduce the load fluctuation, combining with ESS, taking the connection type of ESS as one of the criteria of scenario division, three scenarios are set. The effects of applying ESS is analyzed, and so is the combined wind power and energy storage.

This paper is organized as follows. In Section 2, structure of WEHES is analyzed. In Section 3, the mentioned device operation models of the WEHES are expressed. In Section 4, a WEHES optimization model considering both economic benefits and renewable energy waste is proposed. In Section 5, the proposed model is simulated by an example in North China in the heating season and three simulation scenarios are designed. The operation results are analyzed. Finally, Section 6 gives a brief summary and conclusions.

2. Structure of WEHES

The WEHES includes WPP, PV units, combined heat and power units (CHP) with waste heat boiler, ESS, electric boiler (EB), and heat storage (HS). Among them, CHP is consisted of conventional gas turbine (CGT), waste heat boiler, and gas-fired boiler (GB). CHP has the characteristics of electrothermal coupling output, and can operate in two operation modes, i.e., “power by heat” and “heat by power”. In this paper, due to the various power sources in the MES, CHP is set to follow the mode of “power by heat”. The structure is shown in Figure 1.

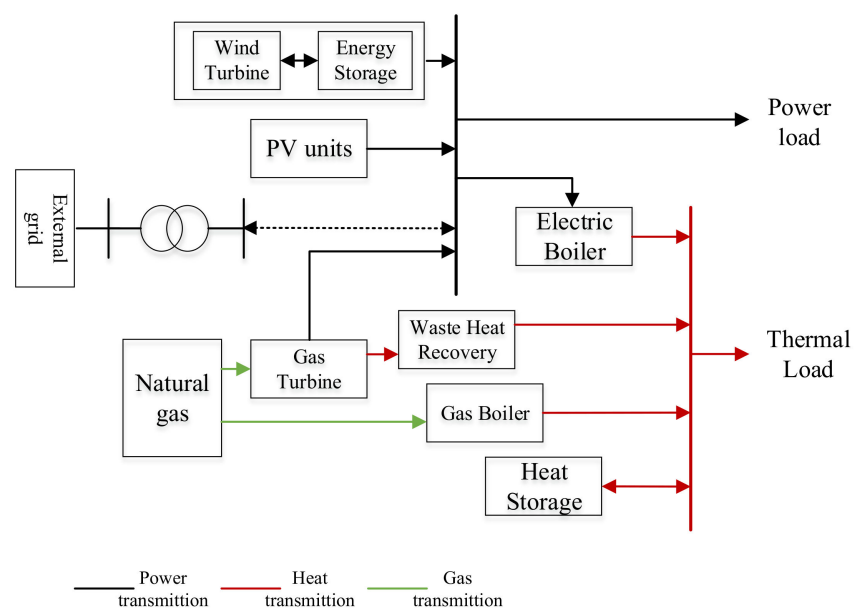


Figure 1. Hybrid energy system (HES) structure.

In the hybrid energy system (HES), renewable energy on the power side, such as wind power, photovoltaic, etc., has great output volatility and uncertainty, which will bring certain operational risks to the distribution network operation when connected to the grid. Therefore, ESS is often applied to stabilize the fluctuation and ensure the stability of the grid. In the WEHES, ESS can suppress the wind power output fluctuation, adjust the output flexibly [24], cut the load peak and fill valley [25], etc. Considering the wind power output in peak and valley periods, lower price or even zero price strategy can be adopted to reduce the wind power curtailment or avoid wind power units shutting down, which further reduces the operation cost and improves the consumption rate of wind power.

In WEHES, wind power and ESS are jointly operated. ESS charges in the spare nighttime when wind power over-produced, and discharges in the peak time, thus can improve the economic benefits through combination. Meanwhile, the combined WPP-ESS shows

better stability on power generation and can participate in auxiliary services in the power market, providing a certain backup for the distributed power in the system. After the combined heat supply network, the excess power can be converted into heat through the electric boiler to meet certain heat load.

3. WEHES Devices Model

3.1. CHP Operation Model

Gas turbine has advantages as small volume, high power output, lower cost, and fewer pollution, so it has been applied in many occasions [26]. Gas turbines can be divided into large, small, and micro gas turbines according to the power scale, ranging from several hundred megawatts to several thousand megawatts. The operation model of CGT is as follows.

$$\begin{cases} P_{tur} = aE_{tur} + b \\ G_{tur} = pE_{tur} + q \\ P_{tur}^{ma} = P_{tur,t_0}^{max} \left[1 - \frac{1}{2}c((t - t_0) + |t - t_0|) \right] \end{cases} \quad (1)$$

wherein P_{tur} represents the generation output of CGT. E_{tur} represents the calorific value of the inputting fuel of CGT. G_{tur} is the available calorific value of CGT.

3.2. Wind Power Plant Generation Model

$$P_W = \begin{cases} 0, & v \leq v_i \\ av^3 - bP_r, & v_i \leq v \leq v_r \\ P_r, & v_r \leq v \leq v_o \\ 0, & v \geq v_o \end{cases} \quad (2)$$

wherein P_W is the wind power output. v_i , v_o , and v_r represent the cut-in wind speed, cut-out wind speed and the rated wind speed, respectively. P_r is the rated power output. a and b are the wind speed correlation coefficients.

3.3. PV Generation Model

Generally, the PV output curve satisfies the β distribution, as follows.

$$f(\theta) = \begin{cases} \frac{\Gamma(\alpha)\Gamma(\beta)}{\Gamma(\alpha+\Gamma(\beta))} \theta^{\alpha-1} (1-\theta)^{\beta-1}, & 0 \leq \theta \leq 1, \alpha \geq 0, \beta \geq 0 \\ 0 & \end{cases} \quad (3)$$

wherein α and β are the shape parameters of β distribution. θ is the radiance correlation coefficient. The average value and standard deviation of irradiance are used to calculate the β parameters through Formulas (4) and (5).

$$\beta = (1 - \mu) \times \left(\frac{\mu \times (1 + \mu)}{\delta^2} - 1 \right) \quad (4)$$

$$\alpha = \frac{\mu \times \beta}{1 - \mu} \quad (5)$$

wherein μ and σ are the mean and normal distribution of solar radiation. The probability of solar radiation state can be obtained by Formula (6).

$$P(\theta) = \int_{\theta_c}^{\theta_d} f(\theta) d\theta \quad (6)$$

wherein θ_c and θ_d are the upper and lower limit of the solar radiation. The solar radiation can be converted into electric power, and the PV output is obtained through Formula (7).

$$g_{m,PV}(t) = \eta_{PV} \times S_{PV} \times \theta_t \quad (7)$$

wherein η_{pv} is the PV power efficiency. S_{pv} is the total surface area of PV modules. θ_t is the radiation time.

3.4. GB Operation Model

The output of gas-fired boiler is closely related to its output characteristics and load, as follows.

$$Q_{GB} = \eta_{GB} F_{GB} \quad (8)$$

wherein Q_{GB} is the heat provided by GB. η_{GB} is the thermal efficiency of GB. F_{GB} is the gas amount require for production of GB.

3.5. Operation Loss of ESS

The loss in the process of ESS operation mainly includes the state switching loss between the shutdown state and the working state (charging/discharging).

$$C_{ESS}(t) = \sum_{t=2}^T [u_c(t)(1 - u_c(t-1)) + u_d(t)(1 - u_d(t-1))] C_{on} \quad (9)$$

wherein $u_c(t)$ and $u_d(t)$ are variables of the charging and discharging state at time t , respectively. C_{on} is the start-up cost of ESS at working state, similar with the start-up and stop cost of the generators.

3.6. Operation Cost of Combined WPP and ESS

In the combination, ESS can assist wind power getting grid-connected. In addition, the extra power in valley periods can be stored and released at peak hours. The operation of the combined WPP and ESS is as follows.

$$P_o = P_W - P_b \quad (10)$$

$$0 \leq P_W \leq \min(P_{Wf}, P_{W,max}) \quad (11)$$

wherein P_W is the wind power output. P_b is the power of ESS, and the states is indicated by whether the value is positive. If $P_b > 0$, the ESS is charging. Otherwise, ESS is discharging. P_{Wf} is the forecasted wind power output. $P_{W,max}$ is the rated power of the WPP.

When dispatching, the dispatching range should be less than the rated power of the WPP, as follows.

$$0 \leq P_{sc} \leq P_{W,max} \quad (12)$$

In actual operation, the wind power has partial priority on grid-connection, and the combined energy storage with the WPP can efficiently save the extra wind power. However, considering the gap between the ultra short-term forecasted load and the actual load demand of power system, certain amount of wind curtailment still happens.

4. WEHES Optimization Model

4.1. Model Construction

Wind power and PV power generation have significant environmental benefits. However, the output uncertainty often leads to the reduction of power grid-connection and power curtailment. The application of ESS, especially under the premise of serious wind curtailment, can effectively reduce the power waste, and increase the system operation cost and, thus, reduce the economic benefits. Therefore, how to balance the power outage and economic benefits is the key to the WEHES operation optimization. In this paper, the multi-objective optimization model of WEHES is proposed with the objectives of maximizing economic benefits and minimizing system energy waste.

(1) maximum economic benefits

The total cost of the system includes the operation costs of WPP, PV, CHP units and DR, and the power purchasing cost with the external grid.

$$obj_1 = \max \sum_{t=1}^T \left(\sum_{i=1}^n p_t^{WPP} * P_{i,t}^{WPP} + \sum_{u=1}^m p_e * P_{u,t}^{PV} + \sum_{t=1}^T p_e * P_t^G + p_H * h_t \right) - \sum_{t=1}^T \left(\sum_{i=1}^n C_i^{WS} (P_{i,t}^{WS}) + C^{GB}(h_t) + C_{pur} + C^{CHP}(P_t^{CHP}, h_t + C_{DR}) \right) \quad (13)$$

$$C^{CHP}(P_t^G, Q_h^{GB}) = a_0 + a_{1,t} P_t^G + a_2 h_t + a_3 (P_t^G)^2 + a_4 h_t^2 + a_5 P_t^G h_t \quad (14)$$

wherein p_e is the power price at time t . $P_{i,t}^W$ shows the output of wind turbine i at time t . $P_{u,t}^{PV}$ represents the PV output at time t . p_H is the heat price. h_t is the heat supply of the gas-fired boiler at time t . C_i^{WS} shows the operation costs of the combined wind power and energy storage. C^{CHP} is the operation cost of CHP. C_{pur} represents the power purchasing fee with the external grid.

(2) Minimum system energy waste

$$obj_2 = \min \sum_{t=1}^T (C_{W,t}^{cur} g_{WPP,t}^{cur} + C_{P,t}^{cur} g_{PV,t}^{cur}) \quad (15)$$

$$g_{WPP,t}^{cur} = g_{WPP,t}^f - g_{WPP,t} \quad (16)$$

$$g_{PV,t}^{cur} = g_{PV,t}^f - g_{PV,t} \quad (17)$$

wherein $C_{W,t}^{cur}$ and $C_{P,t}^{cur}$ are the cost coefficients of the curtailed wind power and PV at time t . $g_{WPP,t}^f$ and $g_{WPP,t}$ are the forecasted power output and real power output of WPP at time t . $g_{PV,t}^f$ and $g_{PV,t}$ are the forecasted power output and real power output of PV at time t .

Considering the weighted coefficient method, the multi-objective problem can be simplified by introducing a comprehensive satisfaction index F . so the objective function can be expressed as follows.

$$\min F = \lambda_1 \frac{f_{1,max} - f_1}{f_{1,max}} + \lambda_2 \frac{f_2 - f_{2,min}}{f_{2,min}} \quad (18)$$

wherein λ_1 and λ_2 are the weighting coefficient of objective 1 and objective 2. $f_{1,max}$ represents the maximum value that can be achieved when objective 1 is applies. $f_{2,min}$ represents the minimum value that can be achieved when only objective 2 is carried out.

4.2. Constraint Conditions

(1) Electric power balancing

$$P_t^{WS} + P_t^{PV} + P_t^{GT} + P_t^{pur} = L_t^E + P_t^{WS} - u_{DR,t} \Delta L_{DR,t} \quad (19)$$

(2) Thermal power balancing

$$Q_{GB,h} + \sum_{i \in CHP} Q_{i,h} \eta_{HX} + Q_{TS0,h} \geq L_h \quad (20)$$

wherein $Q_{GB,h}$ is the heat energy provided by the gas-fired boiler. $\sum_{i \in CHP} Q_{i,h} \eta_{HX}$ represents the heat power of heat-recirculation device. $Q_{TS0,h}$ represents the thermal power of the HS. L_h is the heat load of the system.

(3) CHP operation constraints

The operation constraints of CHP mainly include the output constraints, climbing constraints and start-stop constraints.

$$u_{C,t} P_{C,t} \leq P_{C,max} \tag{21}$$

$$|P_{C,t} - P_{C,t-1}| \leq \Delta P_C \tag{22}$$

$$(T_{C,t-1}^{on} - M_C^{on})(u_{C,t} - u_{C,t-1}) \leq 0 \tag{23}$$

$$(T_{C,t}^{off} - M_C^{off})(u_{C,t-1}, u_{C,t}) \leq 0 \tag{24}$$

wherein $u_{C,t}$ is the status variables of the CHP at time t . $P_{C,min}$ and $P_{C,max}$ are the minimum and maximum output of the CHP under the working condition at time t , respectively. $P_{C,t}$ represents the CHP output at time t . $T_{C,t-1}^{on}$ is the continuous operation time of CHP at time $t-1$. M_C^{on} is the minimum start-up time of CHP. $T_{C,t}^{off}$ is the continuous downtime of CHP at time t . M_C^{off} is the minimum shutdown time of the CHP.

(4) DR operation constraints

With DR, the load curve changes into a smoother shape. In order to avoid the peak-valley inverse distribution of the load, the load curve should be smoothed in the maximum way.

$$|\Delta L_{DR,t}| \leq u_{DR,t} \Delta L_{DR,t}^{max} \tag{25}$$

$$u_{DR,t} \Delta L_{DR}^{Low} \leq \Delta L_{DR,t} - \Delta L_{DR,t-1} \leq u_{PB,t} \Delta L_{DR}^{Up} \tag{26}$$

$$\sum_{t=1}^T \Delta L_{DR,t} \leq \Delta L_{DR}^{max} \tag{27}$$

wherein $\Delta L_{DR,t}^{max}$ represents the maximum load variation at time t . ΔL_{DR}^{Low} and ΔL_{DR}^{Up} are the upper and lower limits of the load variation.

4.3. Solving Method of the WEHES

The objective functions are greatly affected by the distributed wind power and PV. In the optimization, the renewable energy generation can be regarded as a renewable energy decision-maker whose control variable is selected with the aim of obtaining the worst result, the renewable energy consumption level. Meanwhile, the maximum economic benefits can be regarded as the goal of system decision-maker, which is opposite to the decision makers of the renewable energy generation, so that the objective functions can reach the optimal. Moreover, two control variables are coupled and influenced mutually, forming a dynamic gaming process. The system decision-maker wants to optimize the objective function as much as possible based on the renewable energy output strategy, which is a typical robust optimization problem.

On considering the gaming behavior between the two kinds of decision makers, the robust optimization is obtained as shown in Equation (28). The formula is a constrained min-max optimization problem.

$$\begin{cases} \max_{u_1} F(u_1, u_2), \min_{u_2} F(u_1, u_2) \\ s.t. \\ g(u_1, u_2) = 0 \\ h(u_1, u_2) \leq 0 \\ u_1 \in U_1 \\ u_2 \in U_2 \end{cases} \tag{28}$$

wherein u_1 is the control variables for system decision makers and u_2 is the control variables for renewable energy decision makers. $\max_{u_1} F(u_1, u_2)$ represents the intention of the system

decision maker, which is to maximum the system benefits, using u_1 as the only control variable. Similarly, $\min_{u_2} F(u_1, u_2)$ represents the intention of the renewable energy decision makers, which is to minimum the renewable energy waste, using u_2 as the only control variable. $g(u_1, u_2) = 0$ is the equality constraint and $h(u_1, u_2) \leq 0$ is the inequality constraint. U_1 represents the feasible strategy set for system decision makers and U_2 represents the feasible strategy set for the decision maker of renewable energy output.

The specific variables of u_1 and u_2 are shown below.

$$u_1 = [P_{i,t}^W, P_{u,t}^{PV}, C_i^{WS}, C^{CHP}, C_{pur}] \quad (29)$$

$$u_2 = [P_t^W, P_t^{PV}] \quad (30)$$

The two kinds of decision makers finally reach an equilibrium point where neither of them reaches the optimal, but the comprehensive benefits does. Assuming that the equilibrium point is (\bar{u}_1, \bar{u}_2) , neither of the two kinds of decision makers can optimize their objective function further by changing strategies. Then the formula is satisfied by $\forall(u_1, u_2)$.

$$\max_{u_1} F(u_1, \bar{u}_2) \leq \max_{u_1} F(\bar{u}_1, \bar{u}_2) \quad (31)$$

$$\min_{u_2} F(u_1, \bar{u}_2) \geq \min_{u_2} F(\bar{u}_1, \bar{u}_2) \quad (32)$$

It can be seen from the above two equations that, the system decision makers cannot reduce the comprehensive satisfaction further by changing strategies, which also indicates that the renewable energy decision makers cannot improve their comprehensive satisfaction either. Therefore, when the strategy of the system decision makers is u_1 , the response of the distributed energy decision makers to u_1 is $u_2(u_1)$, so the multi-objective function can be transformed to $F(u_1, u_2(u_1))$. However, if the response of the system decision maker to strategy u_2 is $u_1(u_2)$, then $\bar{u}_1 = u_1(u_2(\bar{u}_1))$, which is the equilibrium point.

In addition, the particle swarm optimization (PSO) algorithm is applied to reach the search for the optimal result. In PSO algorithm, each particle represents a potential solution [27–29]. The position, velocity and fitness of the particle are used to measure the quality of the solution. Each particle can move freely. The direction and distance of the movement depend on the speed, which is affected by the experience of its own and the swarm movement. After updating the particle position the fitness is calculated again. The optimal position is obtained by tracking and comparing the individual and group positions.

Suppose in D -dimensional space, the particle swarm contains n particles, which is described as $X = [X_1, X_2, \dots, X_n]$. The vector of particle i in the D -dimensional space is $X_i = [x_{i1}, x_{i2}, \dots, x_{iD}]^T$. The speed of particle i is $V_i = [V_{i1}, V_{i2}, \dots, V_{iD}]^T$. The extremum of individual particle can be expressed as $J_i = [J_{i1}, J_{i2}, \dots, J_{iD}]^T$ and the extremum of the particle swarm is $J_q = [J_{q1}, J_{q2}, \dots, J_{qD}]^T$.

In each iteration, the particle learns from its own extremum and the swarm extremum to update its velocity and position.

$$V_{id,k+1} = \zeta V_{id,k} + r_1 s_1 (J_{id,k} - X_{id,k}) + r_2 s_2 (J_{qd,k} - X_{id,k}) \quad (33)$$

$$X_{id,k+1} = X_{id,k} + V_{id,k+1} \quad d = 1, 2, \dots, D \quad i = 1, 2, \dots, n \quad (34)$$

wherein ζ is the inertia weight. k represents the number of iterations. X_{id} is the position component of particle i . V_{id} is the velocity component of particle i . J_{id} is the extremum component of particle i . J_{qd} is the swarm extremum component. r_1 and r_2 are the acceleration factors, which are both nonnegative constants. s_1 and s_2 are random numbers distributed in $[0, 1]$.

Combined with the model, the solving process is shown in Figure 2.

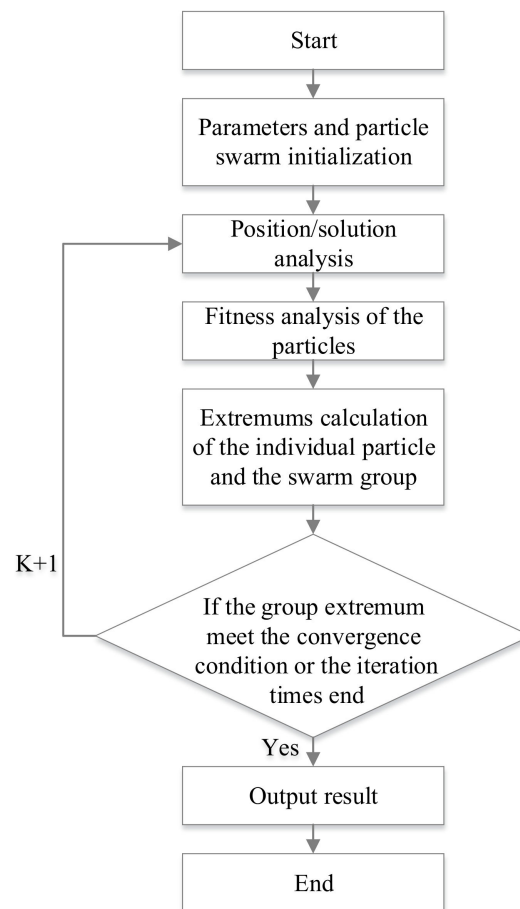


Figure 2. Flow chart of the algorithm.

- (1) Set size of the particle swarm and the maximum number of iterations. Input ζ , r and s , and set accuracy.
- (2) The initial position information of each particle is given.
- (3) The extreme value of the individual particle and the particle swarm are obtained by fitness calculation.
- (4) Update the particle position. The next iteration begins.
- (5) When the number of iterations is exhausted or the result reaches the specified accuracy, the iteration ends and the optimal solution X' is obtained. At this time, the output composition of WEHES system can be obtained.

5. Case Study

5.1. Basic Data

To verify the feasibility and the accuracy of the proposed model, typical wind power and PV output is obtained shown as follows. The cut-in wind speed of WPP is 3 m/s, the rated wind speed 15 m/s, and the cut-out wind speed 25 m/s. The shape parameters and scale parameters are set as $\varphi = 2$, $\theta = 2\frac{\bar{v}}{\sqrt{\pi}}$, and the PV radiation intensity parameters are set as $\alpha = 0.3$ and $\beta = 8.54$ respectively. Combined with the above parameters, 50 groups of WPP and PV output scenarios are simulated, and then reduces the number of scenarios to obtain 10 groups of representative scenarios, and finally takes the expected value as the available wind and PV output, as shown in Figures 2a and 3b shows the loads conditions of the power load and the heat load in a typical day [27].

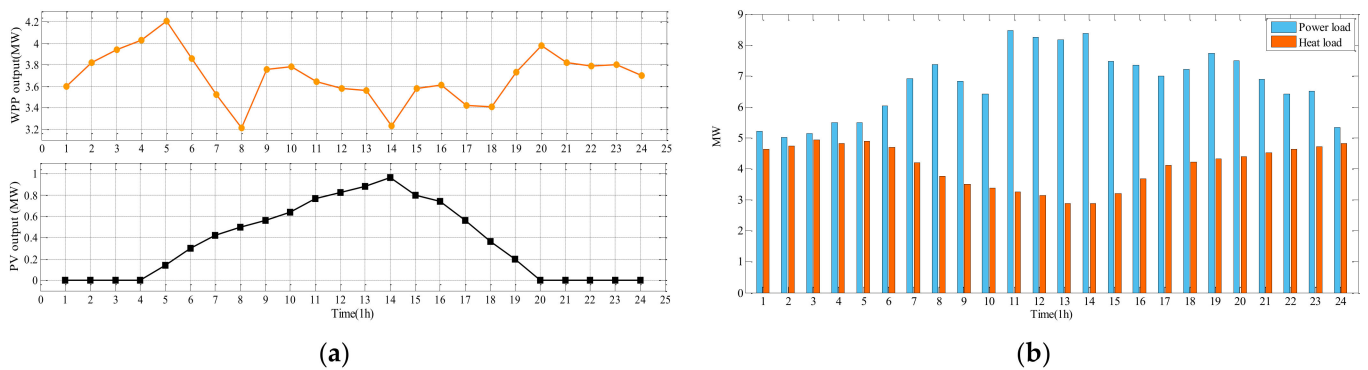


Figure 3. Wind power and PV output (a) and power load and heat load (b).

The time of use (TOU) price mechanism is applied in the WEHES between the power subsystem and the external grid, as shown in Table 1.

Table 1. Price in each period under time-of-use tariff mechanism.

Types	Time Periods	Power Price (Yuan/kWh)
Peak periods	10:00–15:00 and 18:00–21:00	1.25
Valley periods	00:00–07:00 and 23:00–24:00	0.49
Flat periods	the rest time periods	0.86

The gas price equals 2.06 yuan/m³. The energy storage charging/discharging efficiency is 0.95. The self-discharge coefficient of the ESS is 0.01. The capacity of ESS is 5MW [28,29]. The number of particles is set to be 60. The iteration of PSO is 80 times. The initial velocity of the particles are random numbers of [0–1]. ζ decreases with the number of iterations from 0.9 to 0.4 [30–32]. In the calculation process, the iteration times setting as 80.

In the HES, two small wind power plants of 2 MW, one small PV generation cluster of 1 MW and two CGT units of 1 MW are contained. The up and down ramping rates of CGT units are 0.1 MW/h and 0.2 MW/h, and the time-lengths of start-up and shut-down are 0.1 h and 0.2 h, with the start-stop costs of 0.102 ¥/kWh. The cost curve is linearized in two parts with slope coefficients of 110 ¥/MW and 362 ¥/MW and the loss efficiency is 0.052. The self-loss coefficient of the HES is 0.1.

The thermal part mainly consists of the CHP with maximum producing heating power of 4.2 MW. The thermal–electric ratio is 1.2. The operating parameters of CHP unit are set according to literature [29]. The thermal conversion efficiency of EB is 0.90, and the rated power is 1 MW. The loss efficiency of the CHP is 0.052. The price of natural gas is 1.8 yuan/m³. The prices of WPP, PV, and CGT are 0.55 yuan/kWh, 0.75 yuan/kWh, and 0.45 yuan/kWh. After the implementation of DR, the price in normal period remains, with the price in peak period increasing by 10%, and the price in valley period decreasing by 20%.

The maximum electric load and thermal load in the microgrid are 8.057 MW and 4.93 MW respectively, and the region is not involved in carbon emission trading. And the price change situation before and after DR is shown in Figure 4.

5.2. Optimization Results Analysis

Considering the ESS setting, three scenarios are set to analysis the improvement of ESS in HES and the effects of the combined WPP and ESS.

Scenario 1: Basic Scenario. DR is applied in this scenario, but no ESS.

Scenario 2: ESS Scenario. ESS is accessed in the HES.

Scenario 3: Combined WPP and ESS Scenario. The energy storage is combined with the wind power plant, and there is no other ESS in the system to prevent unnecessary cost.

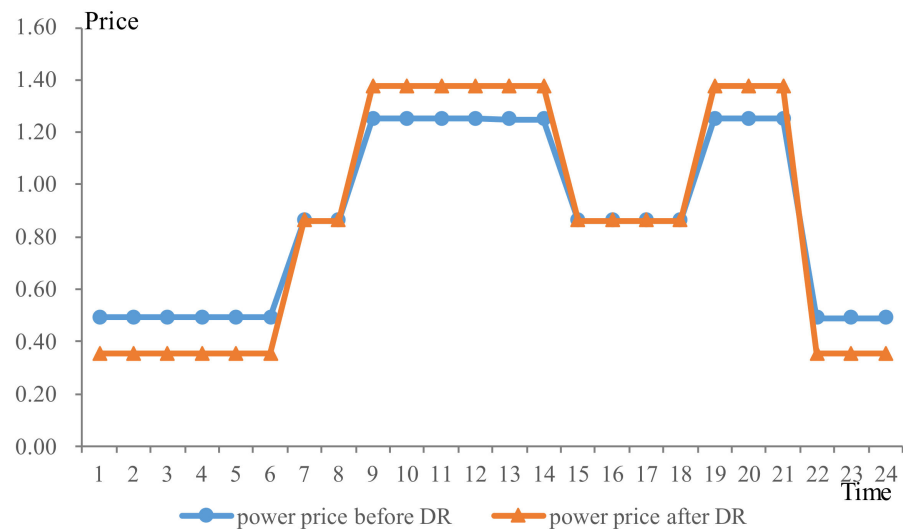


Figure 4. Price curves before and after DR.

5.3. Result Analysis

By introducing DR, the purpose of cutting peak and filling valley can be achieved. After introducing demand response, the load change is shown in the Figure 5.

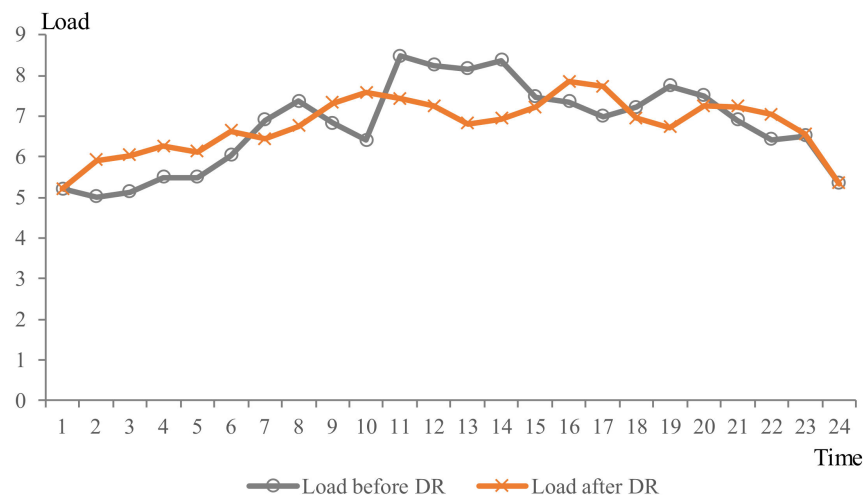


Figure 5. Load changes before and after DR.

(1) Optimization results of scenario 1

As we can see from Figure 6, in scenario 1, the power supply of the HES system is consisted of the WPP, PVs, CHP, and the external grid. The CHP system is composed of conventional gas turbine (CGT), GB, and the waste heat boiler. The power load is met by CHP, WPP, and PV units, and the thermal load is met by CHP, including the wasted heat recovery and the gas-fired boiler, and the electric boiler (EB). In the HES, GB is the main heat supply, CGT is involved in the heating and power supply at the same time, then wind power and PV units provide power, and finally the power gap is satisfied by the external

grid. There is no ESS in the Basic Scenario. The total operation cost is 85,479 yuan, the total cost, containing the purchasing cost and power curtailment cost is 93,940 yuan and the system benefits is 83,128.68 yuan.

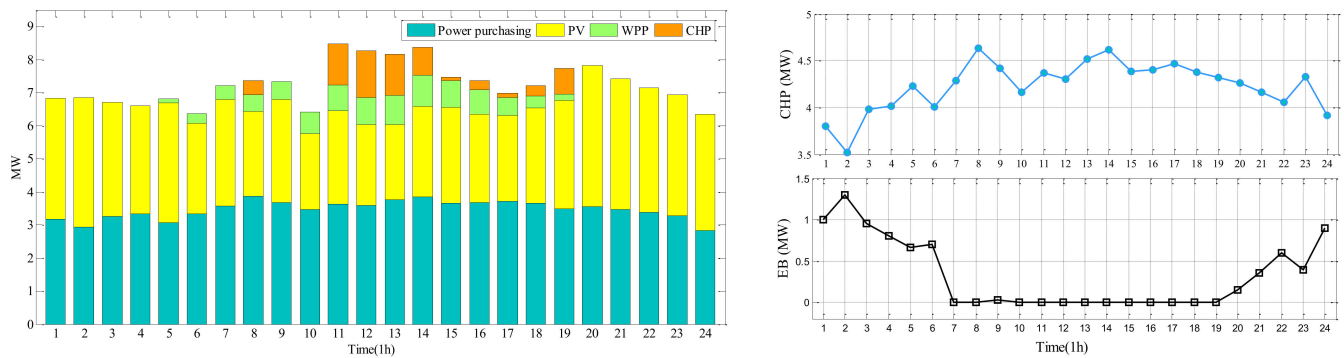


Figure 6. Power supply in Scenario 1 (unit: MW, hour).

(2) Optimization results of scenario 2

As can be seen from Figure 7, compared with Scenario 1, the HES system introduces the ESS in scenario 2. By storing the surplus power in valley hours, higher price at the peak hours can be earned by discharging the stored power.

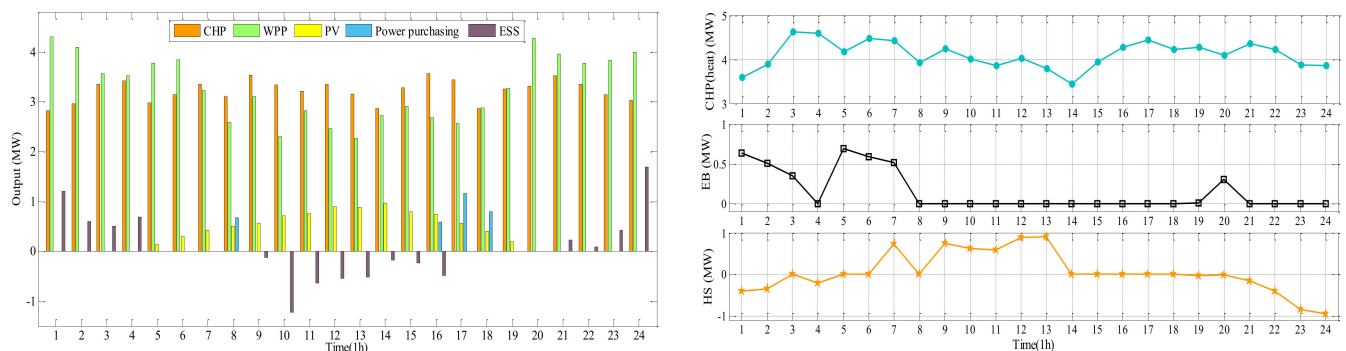


Figure 7. Power supply in Scenario 2 (unit: MW, hour).

During the night-time, WPP generates more power, but the system cannot consume. Through ESS, the excess power of the system can be stored. In addition, considering the higher thermal demand at night, partial electric power can be supplied to the EB to meet the heat demand and reduce the thermal cost. In the peak periods, the ESS discharges. While the heat load in the peak periods is relatively lower. So the HS can operate at day-time to store heat and releases the thermal power at night hours. According to the operation results, the total cost of the Scenario 2 is 78,362.5 yuan and the system benefits of scenario 2 is 104,375.2 yuan.

(3) Optimization results of scenario 3

As can be seen from Figure 8, in scenario 3, considering that the generation capacity of PV units in the system is relatively low, a combined WPP and ESS module is designed to directly store the surplus wind power during the valley period and sell it at a higher price during the peak periods. Similarly, considering the high thermal demand at night, part of the surplus power can be transferred to the EB to provide heating and reduce the thermal cost. In the peak period, the stored power can be released, while the corresponding heat load in the peak period is not high, and the HS can be charged. Based on the whole

operation results, the total operation cost of Scenario 3 is 65,900 yuan, and the system benefits of scenario 3 is 107,546.7 yuan.

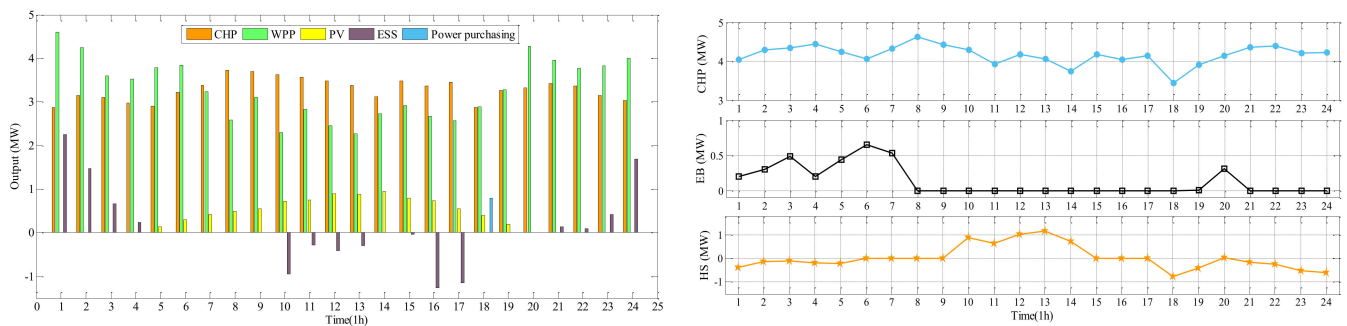


Figure 8. Power supply in Scenario 3 (unit: MW, hour).

(4) Renewable energy consumption comparison

Based on the output results of the three scenarios, the energy output is shown in Table 2.

Table 2. Power generation composition under three scenarios.

Scenarios	WPP	PV	CHP	Power Purchasing
Scenario 1	71.658	8.6	86.25	6.78
Scenario 2	78.726	8.846	77.4	3.227
Scenario 3	79.206	8.846	78.894	0.799

Seen from Table 2, after introducing the ESS, the utilization of renewable energy improves obviously and the power purchasing effectively reduces. In scenario 3, the renewable energy consumption is the highest and the power purchasing is the lowest. That is because the combination of wind power and energy storage improve the consuming ability of wind power, which contributes most in power curtailment. Due to lack of energy storage system, and considering the distribution of wind power output, the excess wind power and PV power is curtailed and the HES in scenario 1 has to purchase power from the external grid, causing extra power purchasing costs.

Considering that PSO is easy to fall into local optimum, the calculation is done 20 times more of each scenario and the average value is obtained. The gap between the calculated results and the mean calculation results is shown in Table 3.

Table 3. Comprehensive comparison between three scenarios.

Index Comparing	Scenario 1	Scenario 2	Scenario 3
Calculated system benefits (yuan)	83,128.68	104,375.2	107,546.7
Mean value of system benefits (yuan)	83,167.73	104,299.4	107,621.0
Calculated power curtailment (MWh)	12.27	2.554	2.507
Mean power curtailment (MWh)	12.29	2.549	2.511

Above all, scenario 3 owns the lowest comprehensive operating cost, and the consumption of wind power and PV can be obtained from the above scenarios. That is because the utilization of the low-price wind power, and the combination of ESS and HS. After applying DR and TOU price mechanism, the power price gap between the valley time and the peak time can bring great benefits through the ESS. In addition, by forming the combined wind power and energy storage, the renewable energy consumption efficiency improves obviously, and achieve the higher system benefits at the same time.

6. Conclusions

Considering the fluctuation influence of renewable energy generation and the power curtailment problem, the application of ESS and the combined WPP and ESS is discussed. By introducing the robust optimization, the proposed multi-objective model of the WEHES is solved, and the following conclusions are obtained.

- (1) The ESS has significant contributions to the reduction of the total system cost. Based on the simulation results, by introducing the ESS, both the power curtailment costs, and the power purchasing costs reduce. By storing the excess wind power at the valley time and discharging at the peak time, more benefits can be gained.
- (2) The combination of WPP and ESS can improve the utilization of wind power to a greater extent and can directly absorb the excess wind power at the valley time and frequency adjustment while getting grid-connection. This combination is more suitable for the hybrid energy system with small proportion of PV power generation.
- (3) The storage and utilization of curtailed wind power is solved by proposed an optimization considering the uncertainty of the incoming wind and the flexible use of ESS, which can be used in the actual situation. However, research on the fluctuation of load side is not profound, which will become a focus of our future research.

Author Contributions: Conceptualization, Z.T. and J.W.; methodology, K.W.; software, Y.L.; validation, J.W., Y.L., and J.Z.; formal analysis, J.W.; investigation, K.W.; resources, Y.L.; data curation, J.Z.; writing—original draft preparation, J.W.; writing—review and editing, Z.T.; visualization, K.W.; supervision, Z.T.; funding acquisition, Z.T. All authors have read and agreed to the published version of the manuscript.

Funding: This research was funded by the 2018 Key Projects of Philosophy and Social Sciences Research, Ministry of Education, China (Project No. 18JZD032).

Institutional Review Board Statement: Not applicable.

Data Availability Statement: This study was not involved this part of content.

Conflicts of Interest: The authors declare no conflict of interest.

References

1. Wang, J.; Zhong, H.; Ma, Z. Review and prospect of integrated demand response in the multi-energy system. *Appl. Energy* **2017**, *202*, 772–782. [[CrossRef](#)]
2. Pu, L.; Wang, X.; Tan, Z.; Wang, H.; Yang, J.C.; Wu, J. Is China's electricity price cross-subsidy policy reasonable? Comparative analysis of eastern, central, and western regions. *Energy Policy* **2020**, *138*, 111250. [[CrossRef](#)]
3. Yang, J.G.; Zhang, N.; Yi, W.; Kang, C. Multi-energy system towards renewable energy accommodation: Review and prospect. *Autom. Electr. Power Syst.* **2018**, *42*, 11–24.
4. De, G.; Tan, Z.F.; Li, M.L.; Huang, L.L.; Song, X.Y. Two-Stage Stochastic Optimization for the Strategic Bidding of a Generation Company Considering Wind Power Uncertainty. *Energies* **2018**, *11*, 3527. [[CrossRef](#)]
5. Ni, L.; Liu, W.; Wen, F. Optimal operation of electricity, natural gas and heat systems considering integrated demand responses and diversified storage devices. *J. Mod. Power Syst. Clean Energy* **2018**, *6*, 423–443. [[CrossRef](#)]
6. Fischer, D.; Harbrecht, A.; Surmann, A.; McKenna, R. Electric vehicles' impacts on residential electric local profiles—A stochastic modelling approach considering socio-economic, behavioral and spatial factors. *Appl. Energy* **2019**, *233*, 644–658. [[CrossRef](#)]
7. Home-Ortiz, J.M.; Pourakbari-Kasmaei, M.; Mantovani, J.R.S.; Lehtonen, M. A mixed integer conic model for distribution expansion planning: Mathuristic approach. *IEEE Trans. Smart Grid* **2020**, *11*, 3932–3943. [[CrossRef](#)]
8. Zeng, D.; Yao, J.; Yang, S. Optimization scheduling model for price-based demand response considering security constraints to accommodate the wind power. *Proc. CSEE* **2014**, *34*, 5571–5578.
9. Wang, K.; Liu, J.T.; Yao, J.G.; Yang, S.C. A Multi-agent Based Interactive Scheduling Model Considering Demand Response. *Power Syst. Autom.* **2014**, *38*, 121–127.
10. Sahand, B.; David, P.C.; Ned, D.; Crawford, C. Interconnection-wide Hour-ahead Scheduling in the Presence of Intermittent Renewables and Demand Response: A Surplus Maximizing Approach. *Appl. Energy* **2017**, *189*, 336–351.
11. Lu, Q.; Chen, T.; Wang, H.; Li, L.; Lu, L.; Li, W.-D. Combined heat and power dispatch model for power system with heat accumulator. *Electr. Power Autom. Equip.* **2014**, *34*, 79–85.
12. Liu, F.; Bie, Z.; Wang, X. Day-ahead dispatch of integrated electricity and natural gas system considering reserve scheduling and renewable uncertainties. *IEEE Trans. Sustain. Energy* **2019**, *10*, 646–658. [[CrossRef](#)]

13. Liu, Y.; Guo, L.; Wang, C. Economic Dispatch of Microgrid Based on Two Stage Robust Optimization. *J. Chin. Electr. Eng. Sci.* **2018**, *38*, 4013–4022.
14. DiSomma, M.; Yan, B.; Bianco, N.; Graditi, G.; Luh, P.B.; Mongibello, L.; Naso, V. Operation Optimization of a Distributed Energy System Considering Energy Costs and Exergy Efficiency. *Energy Convers. Manag.* **2015**, *103*, 739–751. [[CrossRef](#)]
15. Zeng, R.; Li, H.Q.; Liu, L.F.; Zhang, Q.; Zhang, G. A Novel Method Based on Multi-population Genetic Algorithm for CCHP–GSHP Coupling System Optimization. *Energy Convers. Manag.* **2015**, *105*, 1138–1148. [[CrossRef](#)]
16. Guo, Y.; Hu, B.; Wan, L.; Xie, K.; Yang, H.; Shen, Y. Short-term optimal economic operation of thermoelectric power generation microgrid with heat pump. *Autom. Electr. Power Syst.* **2015**, *39*, 16–22.
17. Ma, L.; Liu, N.; Zhang, J.; Tushar, W.; Yuen, C. Energy management for joint operation of CHP and PV prosumers inside a grid-connected microgrid: A game theoretic approach. *IEEE Trans. Ind. Inform.* **2016**, *12*, 1930–1942. [[CrossRef](#)]
18. Zhou, C.; Zheng, J.; Jing, Z.; Wu, Q.; Zhou, X. Multi objective optimization design of integrated energy system for park-level microgrid. *Power Syst. Technol.* **2018**, *42*, 1687–1697.
19. Li, H.; Fang, Y.; Xiao, B. Research on optimized operation of regional integrated energy system considering generalized energy storage. *Power Syst. Technol.* **2019**, *43*, 3130–3138.
20. Gao, H.; Liu, J.; Wei, Z.; Liu, Y.; Wang, W.; Li, X. Multi-scenario two-stage dispatch decision-making model for wind farm with integrated energy storage. *Electr. Power Autom. Equip.* **2014**, *34*, 131–140.
21. Zhao, S.; Wang, Y.; Xu, Y.; Yin, J. Coordinated dispatch of large scale energy storage system and thermal generation in high wind power penetration level system based on chance constrained goal programming. *Proc. CSEE* **2016**, *36*, 969–977.
22. Hu, Z.; Ding, H.; Kong, T. A joint operational model for wind power and pumped-storage plant. *Autom. Electr. Power Syst.* **2012**, *36*, 36–41.
23. Daneshi, H.; Srivastava, A.K. Security-constrained unit commitment with wind generation and compressed air energy storage. *IET Gener. Transm. Distrib.* **2012**, *6*, 167–175. [[CrossRef](#)]
24. Jie, W.; Ming, D. Wind power fluctuation smoothing strategy of hybrid energy storage system using self-adaptive wavelet packet decomposition. *Autom. Electr. Power Syst.* **2017**, *41*, 7–12.
25. Basit, A.; Anca, D.; Altin, M.; Poul, S.; Gamst, M. Compensating active power imbalances in power system with large-scale wind power penetration. *J. Mod. Power Syst. Clean Energy* **2016**, *4*, 229–237. [[CrossRef](#)]
26. Yang, L.; Tai, N.; Fan, C.; Meng, Y. Energy regulating and fluctuation stabilizing by air source heat pump and battery energy storage system in microgrid. *Renew. Energy* **2016**, *95*, 202–212. [[CrossRef](#)]
27. Chen, Y.Z.; He, L.; Li, J. Stochastic dominant-subordinate-interactive scheduling optimization for interconnected microgrids with considering wind-photovoltaic-based distributed generations under uncertainty. *Energy* **2017**, *7*, 581–598. [[CrossRef](#)]
28. Cui, Y.; Chen, Z.; Yan, G.; Tang, Y. Coordinated Wind Power Accommodating Dispatch Model Based on Electric Boiler and CHP With Thermal Energy Storage. *Proc. Chin. Soc. Electr. Eng.* **2016**, *36*, 4072–4081.
29. Torres-Madroño, J.L.; Nieto-Londoño, C.; Sierra-Pérez, J. Hybrid Energy Systems Sizing for the Colombian Context: A Genetic Algorithm and Particle Swarm Optimization Approach. *Energies* **2020**, *13*, 5648. [[CrossRef](#)]
30. Jiang, F.; Peng, Z.J. Forecasting of Carbon Price Based on BP Neural Network Optimized by Chaotic PSO Algorithm. *J. Stat. Inf.* **2018**, *33*, 93–98.
31. Chen, Q.Y.; Chen, W.H.; Dai, C.H.; Zhang, X.X. Reactive Power Optimization Based on Modified Particle Swarm Optimization Algorithm for Power System. *Proc. CSU-EPSA* **2014**, *26*, 8–43.
32. Sun, B.; Yao, H.T. The short-term wind speed forecast analysis based on the PSO-LSSVM predict model. *Power Syst. Prot. Control* **2012**, *40*, 85–89.